http://www.pjbs.org

PJBS

ISSN 1028-8880

Pakistan Journal of Biological Sciences

ANSInet
Asian Network for Scientific Information
308 Lasani Town, Sargodha Road, Faisalabad - Pakistan

OPEN ACCESS Pakistan Journal of Biological Sciences

ISSN 1028-8880
DOI: 10.3923/pjbs.2022.485.494

Research Article
CEG-AgNPs Ameliorates DMBA-Induced Mammary Carcinogenicity by Alleviating Cytokines Expression

[1]Ahmed A. Emara, [1]Ahmed M. Abd Elrahman, [1]Abdelrahman A. Hassan, [1]Ahmed A. Abdelghaney, [1]Ahmed M. Bastawey, [1]Ahmed M. Maher, [1]Abdul-Malik N. Al-Wadayi, [1]Mohamed A. Shalaby, [1]Mohamed M. Mohamed, [1]Mohamed A. Gamal El Din, [1]Saleh A. Muhammad, [1]Ahmed S. Ewees, [1]Mohamed S. Nasr-Eldin, [1]Diana A. Alshrief, [1]Ahmed H. Mohamed, [2]Hala Mostafa, [3]Amr A. El-Ella, [4]Mostafa A. Abdel-Maksoud, [5]Ali A. Ali and [6]Mohammed A. Hussein

[1]Department of Radiology and Medical Imaging, Faculty of Applied Medical Science, October 6th University, October 6th City, Egypt
[2]Department of Medical Laboratories, Faculty of Applied Medical Sciences, October 6 University, Sixth of October City, Egypt
[3]Department of Measurements Photochemistry and Agriculture Applications,
National Institute of Laser Enhanced Science Cairo University, Giza, Egypt
[4]Department of Radiology and Medical Imaging, Faculty of Medicine, Sciences and Technology University, Sudan
[5]Post Graduate Studies, October 6 University, Sixth of October City, Egypt
[6]Department of Biochemistry, Faculty of Applied Medical Science, October 6th University, October 6th City, Egypt

Abstract

Background and Objective: For more than a decade, breast cancer has been one of the most common forms of cancer among women around the world. The present article aimed to evaluate the protective activity of CEG-AgNPs against DMBA-induced mammary carcinoma. **Materials and Methods:** In this experimental study, green synthesis and characterization of CEG-AgNPs were carried as well as IC_{50} against Mcf7 cell line and LD_{50} on mice were evaluated. A total of 24 adult albino mice were divided into four groups six rats in each. Group I was given an equal amount of distilled water, group II was received 80 mg kg^{-1} b.wt., DMBA for 4 weeks, groups III and IV were treated with CEG-AgNPs (28.1 and 70.25 mg kg^{-1}) from the 5th week of DMBA administration for 4 weeks, respectively. **Results:** CEG-AgNPs were approximately 42.32±9.52 nm with a negative zeta potential of -17.44. It is IC_{50} against the Mcf7 cell line and LD_{50} is equal to 82.76 µg mL^{-1} and 1405 mg kg^{-1} b.wt., A significant normalization in plasma ALT, AST, AST and LDH as well as mammary MDA, TNF-α, IL-6, P53, SOD, GPx and GSH levels have been observed in CEG-AgNPs treated mice. Oral CEG-AgNPs administration has suppressed VEGF-C gene expression in DMBA-treated mice. **Conclusion:** The present results, biochemical, histological and MRI results showed that CEG-AgNPs have potent anticancer activity against DMBA-induced mammary carcinoma in mice by inducing the biosynthesizes of antioxidant biomarkers and suppression of cytokines gene expression.

Key words: Cucurbitacin-E-glucoside, dimethylbenz(a)-anthracene, mammary gland, antioxidant enzyme and cytokine storm

Citation: Emara, A.A., A.M. Elrahman, A.A. Hassan, A.A. Abdelghaney and A.M. Bastawey *et al.*, 2022. CEG-AgNPs ameliorates DMBA-induced mammary carcinogenicity by alleviating cytokines expression. Pak. J. Biol. Sci., 25: 485-494.

Corresponding Author: Mohammed Abdalla Hussein, Department of Biochemistry, Faculty of Applied Medical Science, October 6th University, October 6th City, Egypt Tel: 0020124832580

Competing Interest: The authors have declared that no competing interest exists.

Data Availability: All relevant data are within the paper and its supporting information files.

INTRODUCTION

The threat to the health of cancer has grown rapidly[1]. Cancer is the disease group in which cells with potential expansion into other parts of the body have abnormal growth[2].

Not every tumour is cancerous and does not spread to other parts of the body in its beginning. The symptoms and signs include a lump, abnormal bleeding, long cough, unexplained weight loss, etc[3].

Women are now regarded as the world's most common tumour in breast cancer as a global health challenge[4]. Different risk factors include sex, age, a family history, generally inherited mutations, drinking, smoking, obesity and late menopause[5].

Animal carcinogenesis models are reliable and are routinely used for assessing the diagnostic/therapeutic potential of candidate drugs in cancer research[6]. In these models, genomic structural changes take place in three phases, including initiation, promotion and progression[7].

In different cancer tests, chemically induced rodent carcinogenesis is particularly utilized for its high similarity to human cancer concerning histopathology[8].

The 7,12-dimethylbenz (a) anthracene (DMBA) with both carcinogenic and immunosuppressive effects is partly due to enhanced production of prostaglandin E2 (PGE2) have been successfully used to promote mammary tumours in rodent models[9-11].

Cucurbitacins are found in many cucurbitaceous plants. They are most common in species of the Bryonia, Cucumis, Cucurbita, Luffa, Echinocystis, Lagenaria and Citrullus.

Cucurbitacins and their glycosides have been the most studied since, to date, 20 of these highly oxygenated triterpenoids were isolated from the fruit[12,13-18].

These compounds constitute a group of diverse tetracyclic triterpenoid substances, which are well known for their bitterness and toxicity[19]. They possess a broad range of potent biological activities, deriving largely from their cytotoxic and anti-tumour properties[20-22]. Nanotechnology is a rapidly growing field with natural products[23]. The delivery of natural compounds in cancer and other chronic human diseases brings multiple advantages with nanotechnology[24]. The addition, targeting and controlled release profiles of the natural products, of nanoparticles[25-27].

This study presented a simple method for evaluating the anticancer activity of CEG-AgNPs against DMBA-induced mammary carcinoma in mice.

MATERIALS AND METHODS

Study area: The current study was carried out at the Faculty of Applied Medical Sciences, October 6 University, Egypt during September, 2020.

Chemicals and reagents: Cucurbitacin-E-glucoside (95%) and DMBA were purchased from Sigma Chemical Co., St Louis, Missouri, USA. All other chemicals used were of analytical grade.

Synthesis of CEG-AgNPs: The 300 mg of 60 mL Cucurbitacin-E-glucoside was mixed with 10 mL $AgNO_3$ (1 mM) in the presence of a little amount of ethanol then distilled water was added till the total volume of the obtained solution becomes 100 mL. The obtained solution was stirred and heated at 60°C for 10 hrs, after that 200 mL of 40 mM ascorbic acid was added as a catalyst and the brown CEG-AgNPs were suspended and characterized by TEM.

CEG-AgNPs characterization: The X-ray diffraction pattern of CEG-AgNPs was determined at 25-28°C with nickel (Ni) (D8 Advance X-ray diffractometer) filtered using (CuK = 1.54184 A°) radiation as the X-rayed source. The morphology and size of the CEG-AgNPs were studied using a scanning electron microscope and a field transmission microscope at accelerating voltages of 15 and 200 Kv, respectively.

Determination of CEG-AgNPs cytotoxicity on breast carcinoma Mcf7 cell line: Cells were plated into a 24-well plate at a density of 1.0×10^6 cells/well. The particle concentration range was selected based on the minimum concentration showing low toxicity to concentration showing maximum toxicity. The Mcf7 cells were exposed to CEG-AgNPs at a concentration of 31.5, 62.5, 125, 250, 500 and 1000 μg mL^{-1} for 24 hrs. Cells free of particles were used as control cells throughout each assay.

The MTT assay was used to determine the effect of CEG-AgNPs on the viability of Mcf7 cell lines. After exposure, the Mcf7 cells were cultured for 4 hrs with MTT (20 μL/well of 5 mg mL^{-1} stock). Mitochondrial dehydrogenases in living cells convert yellowish water-soluble MTT into water-insoluble formazan crystals that can be dissolved in DMSO. The medium was then withdrawn from each well and 200 μL of DMSO was added to dissolve the formazan crystals. The medium was removed from the suspension culture by centrifugation and then DMSO was added. A microplate reader was used to detect optical density at 570 nm after full mixing (Biotek, USA).

Animals: Female albino mice weighing approximately 35±5 g (84 mice, 60 for LD_{50} estimation and 24 mice for CEG-AgNPs anticancer activity) were obtained from Cairo University's animal house in Giza, Egypt. The animals were kept in a light-controlled room at a temperature of 22°C and a humidity of 55-60%. The animals were kept for a week to acclimate before being fed a standard diet and given unlimited water.

Determination of LD_{50} of CEG-AgNPs: Preliminary tests were performed on groups of four mice. CEG-AgNPs were administered orally in various doses to determine the range of doses that cause 0-100% mortality in animals. The LD_{50} was determined in groups of ten animals by administering resveratrol nanoemulsion at different doses of 500, 800, 1100, 1500, 1700 and 2100 mg kg^{-1} orally. Animals were observed individually every hour for the first day and every day for the next five days following the administration of the tested CEG-AgNPs. Saganuwan's[28] method was used to calculate the LD_{50} using the following Eq.:

$$LSD_{50} = D_m - \left[\frac{\sum(Z.d)}{n}\right]$$

where, D_m is the largest that kill all animals, Σ is the sum of (z×d), Z is the Mean of dead animals between 2 successive groups, d is the constant factor between 2 successive doses and n is the number of animals in each group.

Experimental setup: This experiment was carried out to examine the protective effect of CEG-AgNPs against DMBA-induced mammary carcinoma. The ethical committee of the Faculty of Applied Medical Science, October 6 University was proved the experimental design of the present study. Adult albino mice were divided into four groups with six animals in each. Table 1 describes the test and control groups of the present study.

Blood samples were drawn from each animal's retro-orbital vein and collected in heparin-containing tubes after 30 days of treatment. The heparinized blood samples were centrifuged at 1000 xg for 20 min. Transaminases (L-alanine and L-aspartate)[30], alkaline phosphatase (ALP)[31] and lactate dehydrogenase (LDH)[32] activity were determined using separated plasma.

II-Preparation of mammary samples: The mammary was quickly removed after using cervical dislocation. A portion of each mammary was weighed and homogenized with ice-cold saline in a glass homogenizer (Universal Lab. Aid MPW-309, mechanika precyzyjna, Poland) to make a 25 percent W/V homogenate. The homogenate was prepared in three aliquots. The first was deproteinized with ice-cold 12% Trichloroacetic acid and the supernatant obtained after 1000 xg centrifugation was used to calculate GSH.

The supernatant from the second aliquot was used to calculate the levels of malondialdehyde (MDA), tumour necrosis factor-alpha (TNF-α), interleukin 6 (IL-6) and tumour suppressor P53 (P53). The third aliquot of homogenate was used to prepare a cytosolic fraction of the mammary by centrifuging it at 10500 xg for 15 min at 4°C in a cooling ultra-centrifuge (Sorvall com iplus T-880, Du Pont, USA) and the clear supernatant (cytosolic fraction) was used to determine the activities of SOD and GPx using rat ELISA kit, which is an *in vitro* enzyme-(ELISA). The test was carried out following the supplier's protocol (Rapid, Bio. Laboratories, Inc.).

Quantitative real-time PCR: A TRIzol kit extracted total RNA, 2 µg was reverse transcribed into cDNA. TaqMan one-step PCR Master Mix was used for quantitative real-time polymerase chain reaction (q-PCR) analysis. Total complementary DNA (100 ng/25 µL reaction) was mixed with sequence-specific primers. The cycling conditions of q-PCR assays conditions consisted of 10 min of polymerase activation at 95°C, followed by 40 cycles at 95°C for 15 sec and 60°C for 60 sec and detected by using a StepOne Plus sequence detection system. Normalization of gene expression data used endogenous glyceraldehyde 3-phosphate dehydrogenase as the internal

Table 1: Description of treatment groups

Groups	Group names	Treatment descriptions
I	Normal control A	3 mL of distilled water orally for 30 days
II	DMBA	Mice treated with 80 mg kg^{-1} of DMBA dissolved in sesame oil by oral gavages once a week for 4 weeks[29]
III	DMBA+CEG-AgNPs	Mice treated with 80 mg kg^{-1} of DMBA dissolved in sesame oil by oral gavages once a week for 4 weeks+Oral administration of 1/50 LD_{50} (28.1 mg kg^{-1} b.wt.) CEG-AgNPs in water for 4 weeks from the 5th week of DMBA administration
IV	DMBA+CEG-AgNPs	Mice treated with 80 mg kg^{-1} of DMBA dissolved in sesame oil by oral gavages once a week for 4 weeks+Oral administration of 1/20 LD_{50} (70.25 mg kg^{-1} b.wt.) CEG-AgNPs in water for 4 weeks from the 5th week of DMBA administration

control for mRNA. Gene expression was normalized for relative mRNA in normal healthy tissue and served as the normal control.

The specific primer of VEGF-C: F 5-AACGTGTCCAAGAA ATCAGCC-3, R: 5-AGTCCTCTCCCGCAGTAATCC-3.

The internal control used GAPDH-F: 5-CTCAACTACATGGT CTACATGTTCCA-3 and -R: 5-CCATTCTCGGCCTTGA-CTGT-3.

Histological assessment: For histological examination, the mammary tissues were cut into pieces and fixed in a 10% buffered formaldehyde solution. The fixed tissues were processed with an automated tissue processing machine. Standard techniques were used to embed tissues in paraffin wax. The Hani *et al.*[33], methods was used to prepare 5 mL thick sections that were stained with hematoxylin and eosin for light microscopy analysis. The sections were then examined under a microscope for histopathological changes and photomicrographs were taken.

MRI protocol: MRI was performed on a 9.4 Tesla vertical bore NMR spectrometer (Bruker Biospin, Billerica, MA) equipped with a Micro 2.5 gradient system (100 g cm^{-1} maximum gradient strength), a manufacturer-provided animal imaging probe and a physiological monitoring system (electrocardiograph, respiration and body temperature). A 20 mm diameter volume coil was used as the radiofrequency transmitter and receiver. The temperature was maintained by a heating block built into the gradient system.

Statistical analysis: The results were expressed as mean±SD for each of the eight separate determinations. All the data were statistically analyzed using SPSS/18 software. To test hypotheses, a one-way analysis of variance was used, followed by the least significant difference test ($p \leq 0.05$).

RESULTS

TEM analysis shows that CEG-AgNPs had a size of around 42.32±9.52 nm with a negative zeta potential of +17.44 in Fig. 1.

The sizes and morphology of CEG-AgNPs were systematically investigated using Transmission Electron Microscopy (TEM). TEM images visualize CEG-AgNPs nanoparticles, which exhibit a mean size of 42.32±9.52 nm. CEG-AgNPs samples have spherical shapes with a negative zeta potential of -17.44. Whereas, the surfaces of the CEG-AgNPs were smooth. The discrepancy of CEG-AgNPs might

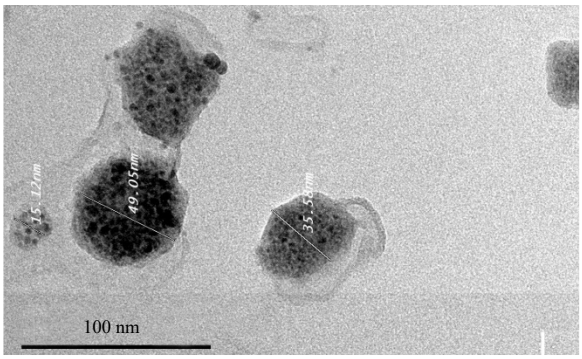

Fig. 1: TEM image (x200) of CEG-AgNPs nanoparticles with a mean size of 42.32±9.52 nm
CEG-AgNPs nanoparticles exhibit spherical shape and smooth surfaces

follow from agglomeration and insufficient redispersion of the primary nanoparticles. This implies that agglomeration takes place with increasing probability the smaller the nanoparticles are, the larger the surface-to-volume ratio (sa/vol) is and the more efficient the attractive interface interactions such as van der Waals forces will become.

The results are reported in Table 2 shows that the incubation of CEG-AgNPs at different consternations (31.25, 62.50, 125, 250, 500 and 1000 µg mL^{-1}) with Mcf7 breast carcinoma cell line resulted in viability % of 100, 50.04, 23.03, 11.77, 4.84 and 4.67, respectively and toxicity % of 0, 49.95, 76.96, 88.22, 95.15 and 95.32, respectively. The IC_{50} value of CEG-AgNPs against Mcf7 cells was 82.76 µg mL^{-1}.

The results are reported in Table 3 shows the oral administration of CEG-AgNPs in doses of 500, 800, 1100, 1500, 1700 and 2100 mg kg^{-1} b.wt., resulted in mortalities of 0, 1, 3, 4, 8 and 10, respectively. The dose of CEG-AgNPs that killed half of the mice (LD_{50}) was 1405 mg kg^{-1} b.wt.

Table 4 shows plasma AST, ALT, ALP and LDH levels. Oral administration of DMBA (80 mg kg^{-1} b.wt.) led to a significant increase in plasma AST, ALT and ALP level as compared to the normal control group ($p<0.05$), indicating acute liver injury. Treatment of animals with CEG-AgNPs (28.1 mg kg^{-1} b.wt.) significantly decreased the level of plasma AST, ALT, ALP and LDH level as compared to the DMBA treated group.

Also, administration of DMBA-treated mice with CEG-AgNPs (70.25 mg kg^{-1} b.wt.) significantly decreased the level of plasma AST, ALT, ALP and LDH level as compared to the DMBA treated group.

Table 5 shows mammary MDA, TNF-α, IL-6 and P53. Oral administration of DMBA (80 mg kg^{-1} b.wt.) led to a significant increase in mammary MDA, TNF-α, IL-6 and P53 as compared to the normal control group ($p<0.05$), indicating acute mammary damage. Treatment of animals with CEG-AgNPs

Table 2: IC_{50} and the effect CEG-AgNPs against Mcf7 breast carcinoma cell line

Nanoparticle	Concentration (μg mL^{-1})	O.D			Mean (O.D)	ST.E	Viability (%)	Toxicity (%)	IC_{50}
CEG-AgNPs	DMSO (0.1%)	0.372	0.399	0.384	0.385	0.00781	100	0	
	1000	0.018	0.018	0.018	0.018	0	4.675324675	95.32467532	82.76
	500	0.019	0.018	0.019	0.018667	0.000333	4.848484848	95.15151515	
	250	0.042	0.036	0.058	0.045333	0.006566	11.77489177	88.22510823	
	125	0.093	0.087	0.086	0.088667	0.002186	23.03030303	76.96969697	
	62.5	0.195	0.182	0.201	0.192667	0.005608	50.04329004	49.95670996	
	31.25	0.382	0.384	0.389	0.385	0.002082	100	0	

OD: Optical density, SE: Standard error

Table 3: Determination of LD_{50} of CEG-AgNPs given orally in adult mice

Group numbers	Dose (mg kg^{-1})	No. of animals/group	No. of dead animals	(Z)	(d)	(Z.d)
1	500	10	0	0.5	300	150
2	800	10	1	2.0	300	600
3	1100	10	3	3.5	400	1400
4	1500	10	4	6.0	200	1200
5	1700	10	8	9.0	400	3600
6	2100	10	10	0	00	6950

$LD_{50} = \left[\frac{\sum(Z.d)}{n}\right]$ $LD_{50} = 2100 - \left[\frac{6950}{10}\right]$ = 1405 mg kg^{-1} b.wt.

Table 4: Effect of CEG-AgNPs on plasma ALT, AST, ALP and LDH activity in mice treated with DMBA

Groups	Treatment descriptions	ALT (U L^{-1})	AST (U L^{-1})	ALP (K U^{-1})	LDH (U L^{-1})
I	Normal control	21.88±3.21^{a}	17.08±2.18^{a}	11.90±1.98^{a}	42.87±4.26^{a}
II	DMBA (80 mg kg^{-1} b.wt.)	57.21±4.99^{d}	47.95±5.60^{d}	35.50±5.70^{d}	173.70±6.33^{d}
III	DMBA (80 mg kg^{-1} b.wt.)+CEG-AgNPs (28.1 mg kg^{-1} b.wt.)	42.06±5.90^{c}	39.73±5.11^{c}	26.30±3.03^{c}	73.12±4.86^{c}
IV	DMBA (80 mg kg^{-1} b.wt.)+CEG-AgNPs (70.25 mg kg^{-1} b.wt.)	32.77±3.80^{b}	23.80±3.07^{b}	17.64±2.60^{b}	52.50±4.40^{b}

Data shown are Mean±Standard deviation of the number of observations within each treatment, Data followed by the same letter are not significantly different at $p \leq 0.05$, ALT: Alanine aminotransferase, AST: Aspartate aminotransferase, ALP: Alkaline phosphatase, LDH: lactate dehydrogenase

Table 5: Effect of CEG-AgNPs on levels of MDA, TNF-α, IL-6 and P53 in mice treated with DMBA

Groups	Treatment description	MDA (nmol mg^{-1} tissue)	TNF-α (pg mg^{-1} tissue)	IL-6 (pg mg^{-1} tissue)	P53 (pg mg^{-1} tissue)
I	Normal control	9.56±1.76^{a}	53.26±5.44^{a}	110.73±9.65^{a}	25.44±5.2^{a}
II	DMBA (80 mg kg^{-1} b.wt.)	57.76±8.66^{c}	243.09±22.80^{c}	583.98±38.50^{c}	108.54±7.65^{c}
III	DMBA (80 mg kg^{-1} b.wt.)+CEG-AgNPs (28.1 mg kg^{-1} b.wt.)	25.49±3.05^{b}	95.27±6.90^{b}	185.09±8.05^{b}	42.77±4.32^{b}
IV	DMBA (80 mg kg^{-1} b.wt.)+CEG-AgNPs (70.25 mg kg^{-1} b.wt.)	19.54±2.17^{a}	61.38±4.82^{a}	137.08±11.73^{a}	32.60±4.98^{b}

Data shown are Mean±Standard deviation of the number of observations within each treatment, data followed by the same letter are not significantly different at $p \leq 0.05$, MDA: Mammary malondialdehyde, TNF-α: Tumour necrosis factor-α, IL-6: Interleukin 6, P53: Tumour suppressor P53

(28.1 mg kg^{-1} b.wt.) significantly decreased the level of mammary MDA, TNF-α, IL-6 and P53 ($p<0.05$) as compared to the DMBA treated group.

Also, administration of DMBA-treated mice with CEG-AgNPs (70.25 mg kg^{-1} b.wt.) significantly decreased the level of mammary MDA, TNF-α, IL-6 ($p<0.05$) as compared to the DMBA treated group.

Table 6 shows a significant decrease in mammary SOD, GPx and GSH level ($p<0.05$) in mice treated with DMBA (80 mg kg^{-1} b.wt.) compared to the control group. The administration of CEG-AgNPs (28.1 mg kg^{-1} b.wt.) showed a significant increase in SOD, GPx and GSH of CEG-AgNPs (70.25 mg kg^{-1} b.wt.) showed a significant increase in SOD, GPx and GSH compared with the DMBA treated group of mice ($p<0.05$).

Figure 2 displayed that DMBA (80 mg kg^{-1} b.wt.) promoted the VEGF-C gene expression in mammary tissues of DMBA-treated mice compared with the control group. Administration of CEG-AgNPs (28.1 and 70.25 mg kg^{-1} b.wt.) significantly ($p<0.05$) led to a statistically significant decrease of VEGF-C gene expression relative to DMBA treated group of mice ($p<0.05$).

Histopathological examination of mammary sections of the normal group (I) showed within normal apparency X400 H and E in Fig. 3a.

On the other hand, in the mammary tissue of DMBA-treated control group (II) histological examination showed marked lobular adenosis (the black arrow), ducts are dilated and showed epitheliosis the circle) and tumorous growth was found in both fibrous tissue and mammary gland X200 H and

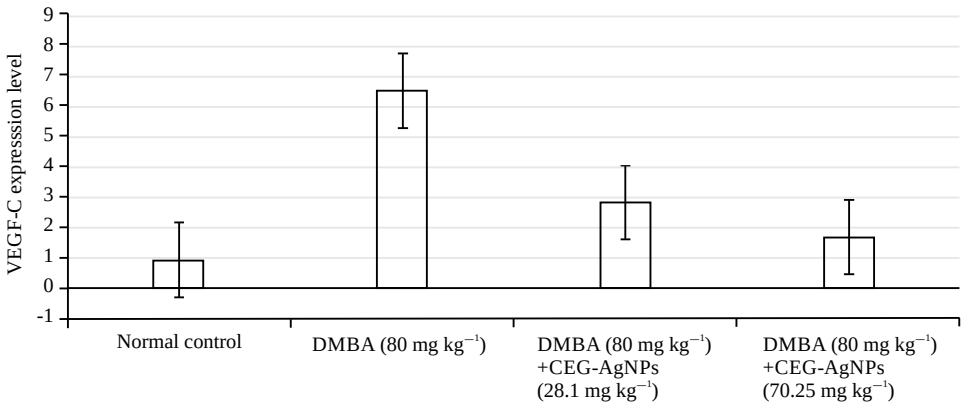

Fig. 2: Effect of CEG-AgNPs (28.1 and 70.25 mg kg^{-1} b.wt.) on levels of mammary vascular endothelial growth factor C (VEGF-C) gene expression in DMBA-treated mice

A representative bar diagram of three independent experiments is presented

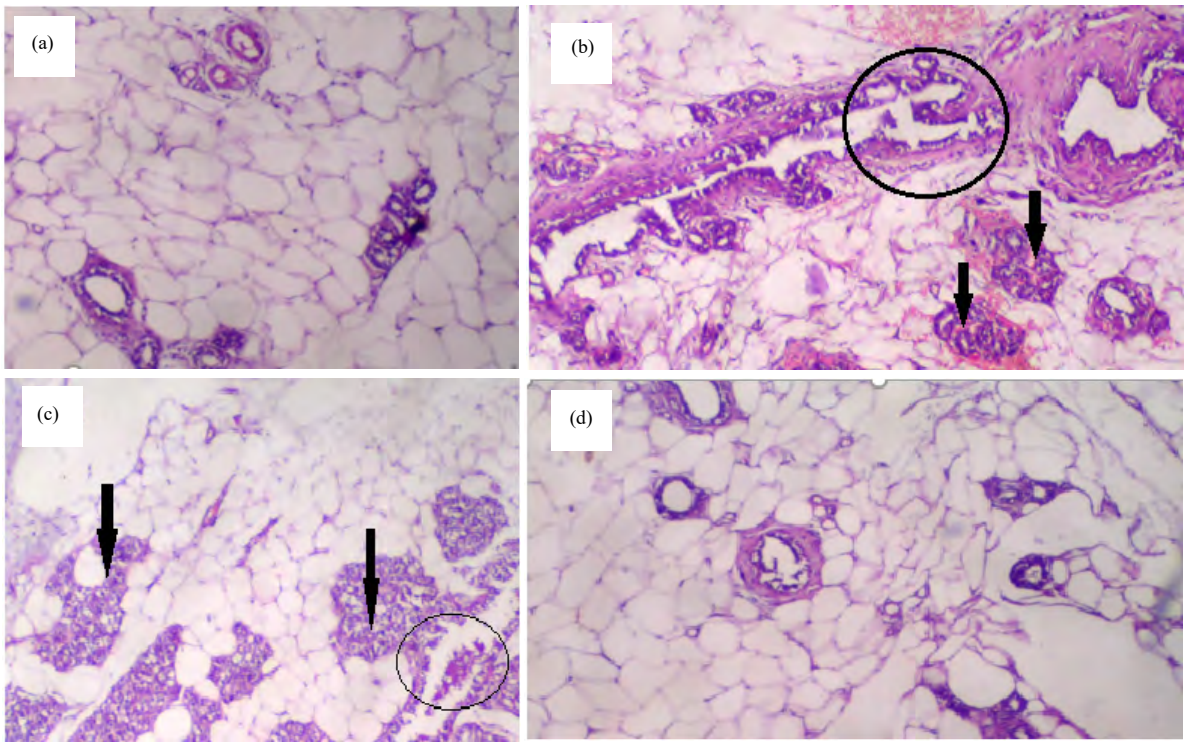

Fig. 3(a-d): Sections stained with hematoxylin and eosin (H and E, 400 X) histological examination of mammary tissues of different groups compared to control group

(a) Group I: Normal control, (b) Group II: DMBA (80 mg kg^{-1} b.wt.), (c) Group III: DMBA (80 mg kg^{-1} b.wt.)+CEG-AgNPs (28.1 mg kg^{-1} b.wt.) and (d) Group IV: DMBA (80 mg kg-1 b.wt.)+CEG-AgNPs (70.25 mg kg^{-1} b.wt.)

E in Fig. 3b. Histopathological examination also showed moderate recovery of DMBA-induced mammary damage by administration of CEG-AgNPs (28.1 mg kg^{-1} b.wt.) as compared to the DMBA-treated mice in Fig. 3c. Fig. 3d, showed crisscross and streaming distribution of fibrocytes and fibroblast cells, which are completely replacing the normal adipose tissue of mammary gland by oral administration of CEG-AgNPs (70.25 mg kg^{-1} b.wt.) against mammary damage induced by DMBA in mice.

MRI examination of mammary tissues of the normal group (I) showed normal architecture of mammary tissue in Fig. 4a.

Table 6: Effect of CEG-AgNPs on levels of mammary SOD, GPx and reduced GSH in mice treated with DMBA

Groups	Treatment description	SOD	GPx	GSH (mg%)
I	Normal control	28.75±2.90^{c}	16.00±1.72^{c}	28.42±3.50^{c}
II	DMBA (80 mg kg^{-1} b.wt.)	14.37±1.64^{a}	5.99±0.65^{a}	14.08±1.09^{a}
III	DMBA (80 mg kg^{-1} b.wt.)+CEG-AgNPs (28.1 mg kg^{-1} b.wt.)	21.04±3.35^{b}	11.32±0.48^{b}	21.45±2.87^{b}
IV	DMBA (80 mg kg^{-1} b.wt.)+CEG-AgNPs (70.25 mg kg^{-1} b.wt.)	26.56±2.06^{c}	16.78±1.27^{c}	27.00±2.67^{c}

Values are given as Mean±SD for groups of six animals each, Values data followed by the same letter are not significantly different at $p \leq 0.05$, SOD: Superoxide dismutase, GPx: Glutathione peroxidase GSH: Reduced glutathione, SOD: One unit of activity was taken as the enzyme reaction, which gave 50% inhibition of NBT reduction in 1 min mg^{-1} protein, GPx: µg of GSH consumed/min mg protein

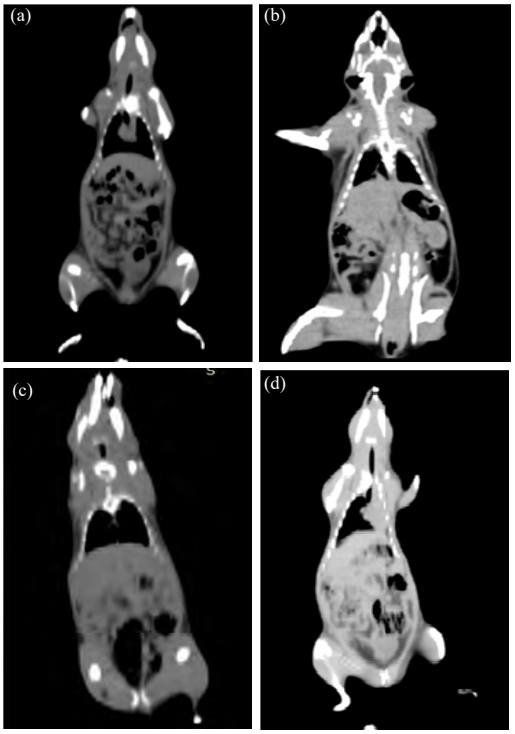

Fig. 4(a-d): Magnetic Resonance Imaging (MRI) examination of mice' mammary tissues of different groups compared to control group
(a) Group I: Normal control, (b) Group II: DMBA (80 mg kg^{-1} b.wt.), (c) Group III: DMBA (80 mg kg^{-1} b.wt.)+CEG-AgNPs (28.1 mg kg^{-1} b.wt.) and (d) Group IV: DMBA (80 mg kg^{-1} b.wt.)+CEG-AgNPs (70.25 mg kg^{-1} b.wt.)

Also, the mammary MRI examination of DMBA-treated mice (II) show fibrous tissues were mostly of mature type and completely replacing the normal adipose tissue of the mammary gland, hence suggestive of mixed mammary tumour in Fig. 4b.

MRI examination also showed coarse texture with moderate improvement in DMBA-treated mice+CEG-AgNPs (28.1 mg kg^{-1} b.wt.) as compared with the DMBA-treated mice (III) in Fig. 4c. In addition, mammary examination by MRI from DMBA-treated mice treated with CEG-AgNPs (70.25 mg kg^{-1} b.wt.) group (IV) showed mammary tissue repair and normal adipose tissue of mammary gland in Fig. 4d.

DISCUSSION

Cucurbitacin-E-glucoside was subjected for the synthesis of CEG-AgNPs and there is the reduction of Ag^{+} ions into silver particles during exposure to Cucurbitacin-E-glucoside which was identified by the change in the colour of the solution to yellowish-brown.

In the present study, CEG-AgNPs was prepared to evaluate their cytotoxicity against the Mcf7 cell line and showed that the IC_{50} = 82.76 µg mL^{-1}. Cucurbitacin and its derivatives are inhibited cancer growth via a wide range of mechanisms, including pro-apoptosis, induction of autophagy, cell cycle arrest, inhibition of cancer invasion and migration[34]. Cucurbitacins also modulate multiple intracellular signalling pathways[35]. Interestingly, each variant of cucurbitacins may trigger slightly different molecular signalling cascades in different cancer cell types to inhibit cancer growth and progress[36].

DMBA The ultimate carcinogen DMBA-3,4-dihydrodiol-1,2-epoxide is formed after metabolic activation by the cytochrome p450 enzyme (DMBA-DE). Various reactive oxygen species are produced during metabolic activity, disrupting the tissue redox equilibrium[37,38]. These reactive species promote the creation of too much LPO in the form of MDA. In both experimental animal models and human cancer patients, high levels of MDA have been widely regarded as an indicator of oxidative stress and antioxidant status[39].

In the present study, there was a significant increase in the plasma AST, ALT and ALP as well as mammary MDA, TNF-α, IL-6 and P53 levels, observed in the DMBA group as compared with the control group. However, in the DMBA+CEG-AgNPs group, the plasma AST, ALT and ALP as well as mammary MDA, TNF-α, IL-6 and P53 levels reduced significantly as compared with the DMBA group. The decreased plasma AST, ALT and ALP as well as mammary MDA, TNF-α, IL-6 and P53 level denotes the antioxidant potential of CEG-AgNPs. The antioxidant potential of CEG-AgNPs may have suppressed of cytokine expression and induction the biosynthesis of antioxidant enzymes[40,41].

Hussein *et al.*[41], reported that Cucurbitacin-E-glucoside has various bioactive effects, including anti-inflammatory and antioxidative activities.

Furthermore, the current study suggested that oral administration of CEG-AgNPs provided significant protection against DMBA-mammary carcinoma via induction of antioxidant enzymes the biosynthesis and suppression of cytokines gene expression. Recent studies reported that cucurbitacin-E-glucoside could alleviate oxidative stress *in vitro* and *in vivo*.

Cucurbitacins are reported to possess significant anti-inflammatory, analgesic[42,43] antioxidant[44], anticancer and gastroprotective activities[45,46].

The efficient recovery of plasma enzymes as well as mammary antioxidant biomarkers and cytokines levels, reflects the therapeutic effects of CEG-AgNPs against the DMBA-induced liver toxicity and mammary carcinoma in mice. The liver protective effect of the CEG-AgNPs was also observed by Hussein *et al*.[41], in LPS-induced-liver toxicity in mice. The observed mammary protective effects of CEG-AgNPs may be due to its antioxidant and anti-inflammatory activity[41].

According to histological and MRI studies, CEG-AgNPs have a mammary protective effect. Because mammary proliferation is an early event in damage-related changes, the attenuation of mammary injury and fibrosis in mice by CEG-AgNPs could be associated with a reduction in the inflammatory response. To the best of my knowledge, the protective effect of CEG-AgNPs against DMBA-induced mammary has never been reported and this study may be the first of its kind.

CONCLUSION

The current study found that CEG-AgNPs have potent protective activity against DMBA-induced mammary damage by normalizing the levels of oxidative stress biomarkers and inflammatory mediator gene expression. Also, current results demonstrated that CEG-AgNPs prevents the liberation of ROS for the damaged tissues by DMBA administration by inhibiting the mammary expression of cytokines and induction of antioxidant biomarkers.

SIGNIFICANCE STATEMENT

This study discovers the protective activity of CEG-AgNPs that can be beneficial for the treatment of DMBA-induced mammary carcinoma. This study will help the researcher to uncover the critical areas that focus on evaluate of CEG-AgNPs as a promising new agent in the treatment of a certain type of cancer that many researchers were not able to explore. Thus, a new theory to explain the correlation between protective activities of CEG-AgNPs and the degree of cytokines suppression in mammary tissue may be arrived at.

REFERENCES

1. Akram, M., M. Iqbal, M., Daniyal and A.U. Khan, 2017. Awareness and current knowledge of breast cancer. Biol. Res., Vol. 50. 10.1186/s40659-017-0140-9.
2. Liu, B., J. Pan and C. Fu, 2021. Correlation of microRNA-367 in the clinicopathologic features and prognosis of breast cancer patients. Medicine, Vol. 100. 10.1097/MD.0000000000026103.
3. Qiao, E.Q., H.J. Yang and X.P. Zhang, 2020. Screening of miRNAs associated with lymph node metastasis in Her-2-positive breast cancer and their relationship with prognosis. J. Zhejiang Uni. Sci. B, 21: 495-508.
4. Ghoncheh, M., Z. Pournamdar and H. Salehiniya, 2016. Incidence and mortality and epidemiology of breast cancer in the world. Asian Pac. J. Cancer Prev., 17: 43-46.
5. Akizawa, Y., T. Kanno, Y. Horibe, Y. Shimizu and E. Noguchi *et al*., 2021. Ovarian metastasis from breast cancer mimicking a primary ovarian neoplasm: A case report. Mol. Clin. Oncol., Vol. 15. 10.3892/mco.2021.2297.
6. Oliveira, P.A., A. Colaco, R. Chaves, H. Guedes-Pinto, P.L.F. De-La-Cruz, and C. Lopes, 2007. Chemical carcinogenesis. Ann. Braz. Acad. Sci., 79: 593-616.
7. Balmain, A. and C.C. Harris, 2000. Carcinogenesis in mouse and human cells: Parallels and paradoxes. Carcinogenesis, 21: 371-377.
8. Currier, N., S.E. Solomon, E.G. Demicco, D.L.F. Chang and M. Farago *et al*., 2005. Oncogenic signaling pathways activated in DMBA-induced mouse mammary tumors. Toxicol. Pathol., 33: 726-737.
9. Miyauchi-Hashimoto, H., K. Kuwamoto, Y. Urade, K. Tanaka and T. Horio, 2001. Carcinogen-induced inflammation and immunosuppression are enhanced in xeroderma pigmentosum group a model mice associated with hyperproduction of prostaglandin E_2. J. Immunol., 166: 5782-5791.
10. Ramadhani, A.H., A.H. Ahkam, A.R. Suharto, Y.D. Jatmiko, H. Tsuboi and M. Rifa, 2021. Suppression of hypoxia and inflammatory pathways by Phyllanthus niruri extract inhibits angiogenesis in DMBA-induced breast cancer mice. Res. Pharm. Sci., 16: 217-226.
11. Bishayee, A. and A. Mandal, 2014. *Trianthema portulacastrum* Linn. exerts chemoprevention of 7,12-dimethylbenz (a)anthracene-induced mammary tumorigenesis in rats. Mutat. Res. Fundam. Mol. Mech. Mutagen., 768: 107-118.
12. Hussain, A.I., H.A. Rathore, M.Z.A. Sattar, S.A.S. Chatha, S.D. Sarker and A.H. Gilani, 2014. *Citrullus colocynthis* (L.) Schrad (bitter apple fruit): A review of its phytochemistry, pharmacology, traditional uses and nutritional potential. J. Ethnopharmacol., 155: 54-66.
13. Song, F., B. Dai, H.Y. Zhang, J.W. Xie, C.Z. Gu and J. Zhang, 2015. Two new cucurbitane-type triterpenoid saponins isolated from ethyl acetate extract of *Citrullus colocynthis* fruit. J. Asian Nat. Prod. Res., 17: 813-818.

14. Nayab, D., D. Ali, N. Arshad, A. Malik, M.I. Choudhary and Z. Ahmed, 2006. Cucurbitacin glucosides from *Citrullus colocynthis*. Nat. Prod. Res., 20: 409-413.
15. Abou-Taleb, N.I., O.A. Elblasy, E.A. Elbesoumy, H.I. Basuny, E.A. Elhamadi and M.S. Nasr Eldin *et al*., 2021. Mechanism of antiangiogenic and antioxidant activity of newly synthesized CAMBA in Ehrlich ascites carcinoma-bearing mice. Asian J. Chem., 33: 2465-2471.
16. Elgizawy, H.A., A.A. Ali and M.A. Hussein, 2021. Resveratrol: Isolation, and its nanostructured lipid carriers, inhibits cell proliferation, induces cell apoptosis in certain human cell lines carcinoma and exerts protective effect against paraquat-induced hepatotoxicity. J. Med. Food, 24: 89-100.
17. Lee, D.H., G.B. Iwanski and N.H. Thoennissen, 2010. Cucurbitacin: Ancient compound shedding new light on cancer treatment. Sci. World J., 10: 413-418.
18. Hussein, M.A., 2011. Synthesis of some novel triazoloquinazolines and triazinoquinazolines and their evaluation for anti-inflammatory activity. Med. Chem. Res., 21: 1876-1886.
19. Maksoud, H.A.A., M.G. Elharrif, M.K. Mahfouz, M.A. Omnia, M.H. Abdullah and M.E. Eltabey, 2019. Biochemical study on occupational inhalation of benzene vapours in petrol station. Respir. Med. Case Rep., 10.1016/j.rmcr.2019.100836.
20. Borik, R.M. and M.A. Hussein, 2021. Synthesis, molecular docking, biological potentials and structure activity relationship of new quinazoline and quinazoline-4-one derivatives. Asian J. Chem., 33: 423-438.
21. Abdel-Gawad, S.M., M.M. Ghorab, A.M.Sh. El-Sharief, F.A. El-Telbany and M. Abdel-Alla, 2003. Design, synthesis and antimicrobial activity of some new pyrazolo[3,4-d] pyrimidines. Heteroatom Chem., 14: 530-534.
22. Luca, A.C., S. Mersch, R. Deenen, S. Schmidt and I. Messner *et al*., 2013. Impact of the 3D microenvironment on phenotype, gene expression, and EGFR inhibition of colorectal cancer cell lines. PLoS ONE, Vol. 8. 10.1371/journal. pone.0059689.
23. Barkat, M.A., Harshita, M. Rizwanullah, F.H. Pottoo, S. Beg, S. Akhter and F.J. Ahmad, 2020. Therapeutic nanoemulsion: Concept to delivery. Curr. Pharm. Des., 26: 1145-1166.
24. Singh, Y., J.G. Meher, K. Raval, F.A. Khan, M. Chaurasia, N.K. Jain and M.K. Chourasia, 2017. Nanoemulsion: Concepts, development and applications in drug delivery. J. Controlled Release, 252: 28-49.
25. S. Parthasarathi, S.P. Muthukumar and C. Anandharamakrishnan, 2016. The influence of droplet size on the stability, in vivo digestion and oral bioavailability of vitamin E emulsions. Food Funct., 7: 2294-2302.
26. Shaban, M.S.A.E.L., D.A. Yousif, N.A. Ahmed, G.R.A. Allah and Y.A. Elbagoury *et al*., 2021. Protective effects of jasonia montana-selenium nanoparticles against doxorubicin-induced liver toxicity. Pak. J. Nutr., 20: 37-45.
27. Mohamed, A.H., M.A.K. Ibrahem, A.A. Elgazar, H.M. Shabib and E.A. Morsy *et al*., 2021. Protective effects of spirulina platensis-selenium nanoparticles against nicotine induced-lung toxicity. Pak. J. Nutr., 20: 9-17.
28. Saganuwan, S.A., 2015. Arithmetic-geometric-harmonic (AGH) method of rough estimation of median lethal dose (LD_{50}) using up and down procedure. J. Drug Metab. Toxicol., Vol. 6. 10.4172/2157-7609.1000180.
29. Karimi, B., M. Ashrafi, T. Shomali and A. Yektaseresht, 2019. Therapeutic effect of simvastatin on DMBA-induced breast cancer in mice. Fundam. Clin. Pharmacol., 33: 84-93.
30. Schumann, G. and R. Klauke, 2003. New IFCC reference procedures for the determination of catalytic activity concentrations of five enzymes in serum: Preliminary upper reference limits obtained in hospitalized subjects. Clin. Chim. Acta, 327: 69-79.
31. Kwon, S.Y. and Y.A. Na, 2014. Serum alkaline phosphatase levels in healthy Korean children and adolescents. Korean J. Clin. Lab. Sci., 46: 79-84.
32. Valvona, C.J., H.L. Fillmore, P.B. Nunn and G.J. Pilkington, 2016. The regulation and function of lactate dehydrogenase A: Therapeutic potential in brain tumor. Brain Pathol., 26: 3-17.
33. Alturkistani, H., F. Tashkandi and Z. Mohammedsaleh, 2016. Histological stains: A literature review and case study. Global J. Health Sci., 8: 72-79.
34. Kim, S.R., H.S. Seo, H.S. Choi, S.G. Cho and Y.K. Kim *et al*., 2013. *Trichosanthes kirilowii* ethanol extract and cucurbitacin d inhibit cell growth and induce apoptosis through inhibition of stat3 activity in breast cancer cells. Evidence-Based Complementary and Altern. Med., Vol. 2013. 10.1155/2013/ 975350.
35. Takahashi, N., Y. Yoshida, T. Sugiura, K. Matsuno, A. Fujino and U. Yamashita, 2009. Cucurbitacin D isolated from *Trichosanthes kirilowii* induces apoptosis in human hepatocellular carcinoma cells *in vitro*. Int. Immunopharmacol., 9: 508-513.
36. Duangmano, S., P. Sae-lim, A. Suksamrarn, F.E. Domann and P. Patmasiriwat, 2012. Cucurbitacin B inhibits human breast cancer cell proliferation through disruption of microtubule polymerization and nucleophosmin/B23 translocation. BMC Compl. Alt. Med., Vol. 12. 10.1186/1472-6882-12-185.
37. Lin, Y., Y. Yao, S. Liu, L. Wang and B. Moorthy *et al*., 2012. Role of mammary epithelial and stromal P450 enzymes in the clearance and metabolic activation of 7,12-dimethylbenz (a)anthracene in mice. Toxicol. Lett., 212: 97-105.
38. Krishnamoorthy, D. and M. Sankaran, 2016. Modulatory effect of *Pleurotus ostreatus* on oxidant/antioxidant status in 7, 12-dimethylbenz (a) anthracene induced mammary carcinoma in experimental rats - a dose-response study. J. Cancer Res. Ther., 12: 386-394.

39. Torun, A.N., S. Kulaksizoglu, M. Kulaksizoglu, B.O. Pamuk, E. Isbilen and N.B. Tutuncu, 2009. Serum total antioxidant status and lipid peroxidation marker malondialdehyde levels in overt and subclinical hypothyroidism. Clin. Endocrinol., 70: 469-474.
40. Tannin-Spitz, T., M. Bergman and S. Grossman, 2007. Cucurbitacin glycosides: Antioxidant and free-radical scavenging activities. Biochem. Biophys. Res. Commun., 364: 181-186.
41. Hussein, M.A., H.A.E. El-Gizawy, N.A.E.K. Gobba and Y.O. Mosaad, 2017. Synthesis of cinnamyl and caffeoyl derivatives of cucurbitacin-eglycoside isolated from citrullus colocynthis fruits and their structures antioxidant and anti-inflammatory activities relationship. Curr. Pharm. Biotechnol., 18: 677-693 10.2174/1389201018666171004144615.
42. Oridupa, O.A. and A.B. Saba, 2012. Relative anti-inflammatory and analgesic activities of the whole fruit, fruit bark, pulp and seed of *Lagenaria breviflora* roberty. J. Pharmacol. Toxicol., 7: 288-297.
43. Marzouk, B., Z. Marzouk, E. Haloui, N. Fenina, A. Bouraoui and M. Aouni, 2010. Screening of analgesic and anti-inflammatory activities of *Citrullus colocynthis* from Southern Tunisia. J. Ethnopharmacol., 128: 15-19.
44. Kumar, S., D. Kumar, M. Jusha, K. Saroha, N. Singh and B. Vashishta, 2008. Antioxidant and free radical scavenging potential of *Citrullus colocynthis* (L.) Schrad. methanolic fruit extract. Acta Pharmaceutica. 58: 215-220.
45. Zhu, Q., M. Zhang, H. Cui, C. Fan, P. Gao, X. Wang and F. Luan, 2017. The complete chloroplast genome sequence of the *Citrullus colocynthis* L. (Cucurbitaceae). Mitochondrial DNA Part B, 2: 480-482.
46. Arawwawala, L.D.A.M., M.I. Thabrew and L.S.R. Arambewela, 2010. Gastroprotective activity of *Trichosanthes cucumerina* in rats. J. Ethnopharmacol., 127: 750-754.